Insights into Kinetics and Isotherms studies of Cadmium (II) adsorption behavior onto wood biochar from aqueous solution

*H. Lalhruaitluanga
Department of Biotechnology
Mizoram University
Aizawl, Mizoram, India
ORCID: 0000-0002-8709-1958

Lalremruata Hauhnar
Department of Zoology
Government Champhai College
Champhai, Mizoram, India
teteahauhnar@gmail.com
ORCID: 0000-0002-7579-6563

Corresponding author*
H. Lalhruaitluanga
Department of Biotechnology
Mizoram University
Aizawl, Mizoram
mahruaia123@gmail.com

DOI: https://doi.org/10.21203/rs.3.rs-3062902/v1.

Abstract

This study aims to investigate the Cd(II) adsorption from aqueous solutions via wood biochar (BC) as an adsorbent, using different parameters such as pH, contact time, and Cd(II) concentration, adsorption isotherms, and kinetic models. To analyze the adsorption mechanism, various isotherms were utilized including Freundlich, Langmuir, Temkin, Redlich-Peterson, Sips, Flory-Huggins, Fowler-Guggenheim, and Harkin-Jura. Additionally, Pseudo-first-order and Pseudo-second-order were used to study the kinetics of adsorption. The Langmuir isotherm suggests that the maximum adsorption capacity (q_{max}) is 28.57 mg/g. According to this model, the metal ions are adsorbed by forming a monolayer and do not interact or compete with each other. Based on the Temkin isotherm, it can be concluded that the adsorption of Cd(II) onto BC is mainly physical in nature, as the value of heat of adsorption is less than 1.0 kcal/mol. The Redlich-Peterson and Sips isotherms indicate that the adsorption process follows the Langmuir form and further supports the monolayer adsorption pattern. The negative value of Gibbs free energy (ΔG^o) suggests that the adsorption process is thermodynamically spontaneous and feasible. The Flory-Huggins and Fowler-Guggenheim isotherms indicate that the active zone of the adsorbent is occupied by adsorbate and also suggest the presence of repulsion between the adsorbate. The kinetics of the adsorption system followed a pseudo-second-order reaction rather than a pseudo-first-order reaction with an R^2 of 0.999 and 0.979, respectively. The results of various analyses indicate that the process of wood biochar adsorption is efficient and can be scaled up for the heavy metals removal from contaminated water.

Keywords: Adsorption, Wood biochar, Cadmium, Isotherms, Kinetics

1. INTRODUCTION

Among all of the heavy metals that are being discharged into the environment, cadmium is one of the most important ones. Because of the high toxicity and persistence of Cd(II) in nature, it has become an increasing concern over the past decades (Liu *et al*., 2019). Long-term exposure to Cd(II) compounds will cause anemia, emphysema, neuralgia, stomach pain, osteoporosis, and other emergencies (Liu *et al*., 2022). Due to its extreme toxicity, Cd(II) needs to be removed from contaminated water to ensure access to safe and pure water. Various techniques have been employed to lower the Cd(II) concentration to meet environmental standards, including chemical precipitation, ionic exchange, adsorption, reverse osmosis, electro-dialysis, ultrafiltration, evaporation. Although these methods perform well, they still have significant disadvantages such as expensive, high sludge production, etc (Zamri *et al*., 2017). Considering the efficiencies and costs of various heavy metal removal methods, adsorption is recommended as a fast and universal treatment technology (Deng *et al*., 2017). Therefore, identifying an affordable and efficient adsorbent for removing Cd(II) is crucial to ensuring the safety of drinking water and food. Various adsorbents are available, biochar (BC), an effective, low-cost, and eco-friendly adsorbent, has been recommended for heavy metal immobilization in wastewater and contaminated soils (Ahmad *et al*., 2014). BC is a carbonaceous solid product and is produced by the pyrolysis of biomass residuals under an oxygen-limited environment. Recently, various types of adsorbent materials such as banana peel biochar (Limmun *et al*., 2024), *Clostridium thiosulfatireducens* (Suya *et al*., 2024), *Ficus virens* (Guo *et al*., 2024), grape stalk (Sabando-Fraile *et al*., 2024), Oyster shell (An *et al*., 2024), sugar cane bagasse (Din *et al*., 2024), etc. have been used for Cd(II) adsorption. In Mizoram, wood BC was used for many purposes such as domestic fuels, pit latrines, water filters, etc. The most preferred wood species to produce BC were Quercus spp., *Mesua ferrea*, *Anogeissus acuminate*, and *Vitex peduncularis* due to their abundant availability in the area and showed the highest wood density (Sahoo *et al*., 2014).

The present study was performed to evaluate wood BC as an adsorbent for the removal of Cd (II) from aqueous solution by systemic evaluation of parameters involved such as pH, contact time, and Cd(II) concentration. Freundlich, Langmuir, Temkin,

Redlich-Peterson, Sips, Flory-Huggins, Fowler-Guggenheim, and Harkin-Jura isotherms were used to study the adsorption mechanism. Similarly, Pseudo- first orders, and Pseudo- second order were used to study the kinetics of adsorption.

2. MATERIALS AND METHODS

2.1. *Wood BC as an adsorbent*

The wood BC was produced by the thermal decomposition of wood at a temperature of 700-800^{o}C under a reduced oxygen supply inside the charcoal kiln. The charring operation can take about 4-5 h. After the charring operation was completed, the wood BC was milled with a blender and sieved to particles of 100 mesh screens.

Preparation of stock solution of metal

All the chemicals used in this study were analytical grade. A stock solution of cadmium (1000 mg/L) was prepared with miliQ water by weighing 2.036 g of $CdCl_2$ (SRL). Different desired concentrations of Cd(II) were prepared by diluting 1000 mg/L of the stock solution. Acid and base solution (1 N HCl and 1 N KOH) were used for pH adjustment. The standard solution of Cd(II) was obtained from SRL.

2.2. *Adsorbent and its characters*

The samples were gold sputter coated and the (SEM) micrographs were taken by using the scanning electron microscope (XL30 ESEM, Philips, USA) to understand the surface morphology of the BC.

2.3. *Batch mode adsorption studies*

The adsorption of Cd(II) ions using wood BC was investigated in a batch mode adsorption equilibrium experiment. All batch experiments were carried out in 100 mL of Cd(II) solution. The effect of pH was evaluated in the range of pH 3.0 – 7.0. The pH of each metal solution was adjusted to the required pH value by using 1 N HCl or 1 N NaOH. Then 0.12 g of dried biosorbent was added to the metal solution. The reaction mixture was shaken for at 150 rpm, 29 ^{o}C for 6 h. Similarly, contact time (15-360 min) and Cd(II) concentration (10-50 mg/L) were also conducted. At the end of the experiment, the solutions were separated from the adsorbent by centrifuging at 10,000

rpm for 8 min. The concentrations of metal were analyzed using MP-AES element analysis, calibrated with a standard solution. The experiment was conducted in triplicate and the average values were used in this data analysis. The amount of Cd(II) adsorbed onto BC at equilibrium, q_e (mg/g), was calculated by the following Equation:

$$q_e = (C_i - C_e) \times V/W \quad (1)$$

where C_i and C_e are the initial and equilibrium liquid-phase concentrations of Cd(II), respectively (mg/L), V is the volume of the solution (L), and W is the weight of the adsorbent used (g)

3. RESULTS AND DISCUSSION

3.1. *Adsorbent and its characters*

SEM micrograph reveals that there are many pores on the surface of the adsorbent. The smaller pore size diameter of 1.36 µm and the bigger pore size is 16.3 µm in diameter (Fig. 1). Different pore sizes in the adsorbent can increase the adsorption process by increasing surface area.

3.2. *Effect of pH*

The adsorption of cadmium was found maximum at pH 6 and lowest at pH 3 as shown in Fig. 2(a). At low pH, there was a high H^+ ions concentration, which competed with Cd(II) for a binding site at the surface of the negatively charged adsorbent, resulting in the decrease of Cd(II) adsorption. As the pH increases, metal adsorption also increase since ion exchange is more effective when fewer H^+ ions are available to compete with the metal ions for binding sites onto the BC surface and reached equilibrium at pH 6. At higher pH, the divalent cationic forms decrease, and more soluble or insoluble hydroxylated forms of cadmium increase (Goswami and Phukan, 2017). The formation of hydroxylated complexes of the metal would also compete with metal ions for the binding sites; as a result the retention decrease again.

3.3. *Effect of initial metal concentration*

The effect of initial metal concentration was studied in the range of 10 – 50 mg/L at 29 ^oC and pH 6. Cd(II) removal range from 86.53% to 43.46 % as shown in Fig. 2(b).

The percentage of Cd(II) adsorption decreased with an increase in Cd(II) ions concentration and showed little decrease in percentage (%) of adsorption at higher concentration. This can be explained that all the adsorbents have a limited number of active sites for Cd(II) to bind, which would become saturated at a certain concentration. So, an increase in initial metal concentration does not increase the sorption process.

3.4. *Effect of time*

The effect of contact time was determined at an initial Cd(II) concentration of 20 mg/L at pH 6. The rate of adsorption was rapid initially and then gradually diminished to attain an equilibrium state at 360 min as shown in Fig. 2(c). The initial fast adsorption is due to the availability of abundant vacant active sites on the adsorbent. The number of active sites in the system is fixed and each active site can absorb only one ion, therefore metal uptake by the sorbent surface is rapid initially and then decreases as the availability of active sites decreases

3.5. *Adsorption isotherm studies*

The Cd(II) uptake capacity on the wood BC at different concentrations (10-50 mg/L) on a fixed amount of adsorbent at pH 6.0 has been evaluated using different adsorption isotherm models.

3.5.1. *Freundlich isotherm*

The Freundlich isotherm (Freundlich, 1907) assumes that monolayer sorption with a heterogeneous energetic distribution of active sites, accompanied by an interaction between adsorbed molecules. Its isotherm is represented by the following Equation 2.

$$\log q_e = \log K_f + (1/n) \log C_e \quad (2)$$

where C_e (mg/L) is the equilibrium concentration, q_e (mg/g) is the amount of metal ions adsorbed at equilibrium, K_f (mg/g) and '*n*' are adsorption capacity and intensity of adsorption, respectively. A graph was plotted $\log q_e$ versus $\log C_e$ as shown in Fig. 3(a). The slopes and intercepts of the graph were used to calculate the *n* and K_f values

(Table 1). If n = 0 to 10, the sorption process is favorable (Ahmadi *et al*., 2020). Therefore, the '*n'* value is within this range indicating the favorability of an adsorption process.

3.5.2. *Langmuir isotherm*

The Langmuir isotherm (Langmuir, 1916) assumes that there is no interaction between adsorbed species and a monolayer was formed when the equilibrium was attained. Its linear form is as follows:

$$C_e/q_e = 1/q_{max}b + C_e/q_{max} \quad (3)$$

where q_{max} (mg/g) is the maximum adsorption capacity and b (/mg) is the energy of adsorption. A graph was plotted C_e/q_e versus C_e with high R^2 value as shown in Fig. 3(b). The slopes and intercepts of the graph were used to calculate the q_{max} and b. The values of q_{max} and b agree well with the theoretical q_e value as shown in Table 1. This indicates that the adsorbed metal ions do not interact or compete with each other and that they are adsorped by forming a monolayer.

3.5.3. *Temkin Isotherm*

The Temkin isotherm (Temkin, 1940) is used for the determination of physical or chemical sorption. Its linear mathematical form is as follows:

$$q_e = B\ln A_T + B\ln C_e \quad (3)$$

where B is defined by the expression $B=RT/b_T$, T is the absolute temperature in Kelvin (K); R is the gas constant (8.314 J/mol K); b_T is the heat of sorption (J/mol); and A_T is the Temkin isotherm constant (L/g). A graph was plotted q_e vs $\ln C_e$ with high R^2 value (Fig. 3c). The slopes and intercepts of the graph were used to calculate the b_T and A_T (Table 1). According to the Tempkin isotherm model, physical adsorption occurs if the heat of the adsorption (b_T) value is less than 1.0 kcal/mol. Furthermore, with a value of 20–50 kcal/mol, chemisorption occurs. If value is between the two (1–20 kcal/mol), both physisorption and chemisorption are involved (Ettish *et al*., 2021). The adsorption of Cd(II) onto BC is predominantly physical adsorption since the heat of adsorption value is less than 1.0 kcal/mol.

3.5.4. *Redlich - Peterson (R-P) Isotherm*

The R-P (Redlich and Peterson, 1959) equation contains three parameters and incorporates the features of the Langmuir and Freundlich isotherms. The R-P isotherm can be described as follows:

$$q_e = K_{RP}C_e/1 + a_{RP}C_e^{\beta} \quad (5)$$

where K_{RP}, a_{RP}, and β are the R-P parameters. A non-linear graph was plotted C_e versus q_e as shown in Fig. 4(a) and the three parameters of R-P isotherm were calculated. β lies between 0 and 1, if β=1, the R-P equation converts to Langmuir form. The calculated β value is very close to unity than "0" with a high regression coefficient (R^2) value (Table 1). This indicates that the adsorption process is following the Langmuir form and further supports the predominance of monolayer adsorption.

3.5.5. *Sips Isotherm*

The Sips isotherm also called the Langmuir-Freundlich isotherm equation is characterized by the heterogeneity factor, "n" and is employed to describe the heterogeneity of sorbent surface if $0 < n < 1$. The isotherm can be expressed as:

$$q_e = q_m K_{LF}C_e^{n}/1 + K_{LF}C_e^{n} \quad (6)$$

where q_m and K_{LF} are the Sips maximum adsorption capacity (mg/g) and Sips equilibrium constant (L/mg), respectively. The value of n is employed to describe the system's heterogeneity, when n is between 0 and 1. When $n = 1$, the Sips equation reduces to the Langmuir equation and implies a homogeneous adsorption process (Allen *et al.*, 2004). A non-linear graph was plotted C_e versus q_e as shown in Fig. 4(b). The parameters of Sips isotherm were calculated, and the value of n is calculated as 1.05, i.e. ≈1 with high R^2 value. This indicated that the adsorption pattern follows Langmuir isotherm and the estimated q_m value is also very close to the q_m value obtained according to Langmuir isotherm (Table 1).

3.5.6. *Flory-Huggins Isotherm*

The Flory-Huggins isotherm was used to evaluate the degree of surface coverage characteristics of adsorbate on the adsorbent and is expressed in its linear form by the following equation 7 (Chaba and Nomngongo, 2019):

$$\ln(\theta/C_i) = \ln K_{FH} + n_{FH}\ln(1-\theta) \quad (7)$$

where θ = (1 - C_e/C_i) is the degree of surface coverage, K_{FH} (L/mol) and n_{FH} represent the Flory-Huggins equilibrium isotherm constant and model exponent, respectively. A linear plot of ln (θ/C_i) versus ln (1 – θ) as shown in Fig. 5(a), K_{FH} and n_{FH} values can be calculated (Table 1). According to the model, If n_{FH} >1, indicates multilayer adsorption of molecules on the adsorbent surface, if n_{FH} < 1, indicates an active zone of the adsorbent would be occupied by adsorbate. Therefore, the calculated value of n_{FH} is less than unity, which indicates that the active zone of the adsorbent is occupied by adsorbate. In addition, the values K_{FH} is used to calculate of spontaneity Gibbs free energy (ΔG^o) (Foo and Hameed, 2010). The negative value of ΔG^o (Table 1) indicates that the adsorption process is thermodynamically spontaneous and feasible.

3.5.7. *Fowler-Guggenheim isotherm*

The Fowler and Guggenheim (Fowler and Guggenheim, 1939) explain whether the lateral interaction between adsorbed molecules in the solid phase existed or not. The linearized form of this model is expressed as:

$$\ln C_e(1-\theta)/\theta = -\ln K_{FG} + 2W\theta/RT \quad (8)$$

where K_{FG} is the Fowler-Guggenheim equilibrium constant (L/mg), W is the interaction energy between adsorbed molecules (kJ/mol), R is the universal gas constan and T is the absolute temperature (K). From a linear plot of $\ln C_e(1-\theta)/\theta$ versus θ as shown in Fig. 5(b), W and K_{FH} can be calculated (Table. 1). According to this model, if W value is positive, the interaction between the adsorbed molecules is attractive. On the other hand, if W is negative, the interaction among adsorbed molecules is repulsive. If W is

equal to 0, there is no interaction between adsorbed molecules. Therefore, the calculated value of *W* is negative, which indicates the presence of repulsion between the adsorbed molecules and the high R^2 value indicates the existence of a monolayer on the surface of the adsorbent (Ragadhita and Nandiyanto, 2021)

3.5.8. *Harkin-Jura Isotherm*

The Harkin-Jura isotherm model (Harkins and Jura, 1944) assumes the possibility of multilayer adsorption on the surface of absorbents having heterogeneous pore distribution. This model is expressed as follows:

$$1/q_e^2 = B/A - (1/A) \log C_e \quad (9)$$

The plot of $1/q_e^2$ versus $\log C_e$ gave a correlation coefficient of 0.761 as shown in Fig. 5(c) with the *A* and *B* values, as Harkin-Jura Isotherm model constants (Table 1). The R^2 value was lesser than that of monolayer adsorption models of Langmuir and could not be the best fit for the adsorption. This indicates that the multilayer adsorption process is not followed.

3.6. Sorption kinetics studies

To explain the kinetics mechanism of Cd(II) sorption and the potential rate-controlling steps, Pseudo-first-order and Pseudo-second-order were used.

3.6.1. Pseudo-first-order

The Pseudo-first-order model (Lagergren, 1898) for solid/liquid systems of adsorption stated that the rate is proportional to the number of unoccupied sites. It is expressed as:

$$\log(q_e - q_t) = \log q_e - k_1\, t/2.303 \quad (10)$$

where q_e and q_t are the amounts of cadmium adsorbed on the adsorbent at equilibrium and at any time t, respectively. k_1 is the rate constant of pseudo-first-order sorption. The slopes and intercepts of a plot of log ($q_e - q_t$) versus *t* (Fig. 6a) were used to calculate

the first-order rate constant, k_1 = 39.15x10^{-3} /min and equilibrium adsorption capacity, q_e.= 13.03 mg/g with the R^2 value of 0.979 .

3.6.2. Pseudo-second-order

The Pseudo-second-order (Ho and Mc Kay, 1999) assumes that the rate of sorption is proportional to the square of the number of unoccupied sites. It is expressed as:

$$t/q_t = 1/k_2 q_e^2 + t/q_e \quad (11)$$

where k_2 is the equilibrium rate constant. The slopes and intercepts of plots t/q_t versus t (Fig. 6b) were used to calculate the pseudo-second-order rate constants, k_2 = 6.42x10^{-3} g/mg/min and q_e = 16.66 mg/g.

The correlation coefficient (R^2) of the pseudo-second-order kinetics model is 0.999 and the experimental q_e values of 16.18 mg/g were also agreed well with the calculated q_e values of 16.66 mg/g, respectively as shown in Table 2. The correlation coefficients of a pseudo-first-order kinetics model were lower than the pseudo-second-order kinetics model. Therefore, it can be concluded that this adsorption system followed a pseudo-second-order reaction rather than a pseudo-first-order reaction.

CONCLUSIONS

The purpose of this study was to evaluate the effectiveness of wood-based biochar as an adsorbent for removing Cd(II) from an aqueous solution. Various adsorption isotherms and Kinetics models were utilized to explain the mechanism of adsorption. Based on the results, it can be concluded that wood-based biochar is a highly efficient adsorbent for removing Cd(II) from an aqueous solution and could be scaled up to remove heavy metals from contaminated water.

ACKNOWLEDGEMENTS

The author gracefully acknowledged the MZUBioNEST, Mizoram University for allowing us to utilize instrument facilities.

CONFLICT OF INTEREST

The authors have no relevant financial or non-financial interests to declare.

FUNDING

The authors declare that no funds or grants were received during the preparation of this manuscript.

REFERENCES

Ahmad, M., Rajapaksha, A.U., Lim, J.E., Zhang, M., Bolan, N., Mohan, D., Vithanage, M., Lee, S.S., and Ok, Y.S., 2014, BC as a sorbent for contaminant management in soil and water: a review, *Chemosphere*. 99:19-33. https://doi. org/10.1016/j.chemosphere.2013.10.071.

Ahmadi, S., Mohammadi, L., Rahdar, A., Rahdar, S., Dehghani, R., Igwegbe, C.A., and Kyzas, G.Z., 2020, Acid Dye Removal from Aqueous Solution by Using Neodymium(III) Oxide Nanoadsorbents, *Nanomater*. 10:556. https://doi.org/10.3390/nano10030556.

Allen, S.J., Mckay, G., and Porter, J.F., 2004, Adsorption isotherm models for basic dye adsorption by peat in single and binary component systems, *J. Colloid Interface Sci.* 280:322–333. https://doi.org/10.1016/j.jcis.2004.08.078.

An, W., Liu, Y., Chen, H., Wang, Q., Hu, X., and Di, J., 2024, Oyster shell-modified lignite composite in globular shape as a low-cost adsorbent for the removal of Pb2+and Cd2+from AMD: Evaluation of adsorption properties and exploration of potential mechanisms, *Arab. J. Chem*. 1:105732. https://doi.org/10.1016/j.arabjc.2024.105732.

Chaba, J.M., and Nomngongo, P.N., 2019, Effective adsorptive removal of amoxicillin from aqueous solutions and wastewater samples using zinc oxide coated carbon nanofiber composite, *Emerg. Contam*. 5:143-149. https://doi.org/10.1016/j.emcon.2019.04.001.

Deng, J., Liu, Y., Liu, S., Zeng, G., Tan, X., Huang, B., Tang, X., Wang, S., Hua, Q., and Yan, Z., 2017, Competitive adsorption of Pb(II), Cd(II) and Cu(II) onto

chitosanpyromellitic dianhydride modified BC, *J. Colloid Interface Sci*. 506:355-364. https://doi.org/10.1016/j.jcis.2017.07.069.

Din, M.I., Mujahid, A., Bock, U., Khalid, R., and Hussain, Z., 2024, A kinetic and thermodynamic investigation for adsorption of cadmium (ii) ions on the microwave modified sugar cane bagasse. *Desalin. Water Treat*. 317:100194. https://doi.org/10.1016/j.dwt.2024.100194.

Ettish, M.N., Gharieb, E., Mohamed. E.A., and Osama, A., 2021, Preparation and characterization of new adsorbent from Cinnamon waste by physical activation for removal of Chlorpyrifos, *Environ. Chall*. 5:100208. http://dx.doi.org/10.1016/j.envc.2021.100208.

Foo, K.Y., and Hameed, B.H., 2010, Insights into the modeling of adsorption isotherm systems. *Chem. Eng. J*. 156:2-10. https://doi.org/10.1016/j.cej.2009.09.013.

Fowler, RH., and Guggenheim, E.A., 1939, Statistical Thermodynamics, Cambridge University Press, London, p. 431-450

Freundlich, H., 1907, Ueber die adsorption in loesungen, *Z. Phys. Chem*. 57:385-470.

Goswami, M., and Phukan, P., 2017, Enhanced adsorption of cationic dyes using sulfonic acid modified activated carbon, *J. Environ. Chem. Eng*. 5:3508–3517. https://doi.org/10.1016/j.jece.2017.07.016.

Guo, M., Jin, T., Wen, L., Wang, B., Lin, J., Li, W., and Deng, H., 2024, Cd(II) and Pb(II) adsorption in karst soils amended with litter extract from *Ficus virens*, *Arab. J. Chem*. 17:105685. https://doi.org/10.1016/j.arabjc.2024.105685.

Harkins, W.D., and Jura, G., 1944, Surfaces of Solids. XI. Determination of the Decrease (π) of Free Surface Energy of a Solid by an Adsorbed Film, *J. Am. Chem. Soc*. 67:1356-1362. http://dx.doi.org/10.1021/ja01236a046.

Ho, Y.S., and Mc Kay, G., 1999, Pseudo-second order model for sorption process. *Proc. Biochem*. 34:451-465. https://doi.org/10.1016/S0032-9592(98)00112-5.

Lagergren, S., 1898, About the theory of so-called adsorption of soluble substances, *Kongl. Vetensk. Acad. Handl*. 241:1-39.

Langmuir, I., 1916, The constitution and fundamental properties of solids and liquids, *J. Am. Chem. Soc*. 38:2221-2295.

Limmun, W., Limmun, W., Borkowski, J.J., Ishikawa, N., Pairintra, R., Chungcharoen, T., Phanchindawan, N., Maneesri, W., Pewpa, O., and Ito, A., 2024, Eco-friendly magnetic biochar from Leb Mu Nang banana peel: Response surface methodology optimization for Cd(II) adsorption from synthetic wastewater, *Bioresour. Technol. Rep*. 25:101743. https://doi.org/10.1016/j.biteb.2023.101743.

Liu, L., Peng, Q., Qiu, G., Zhu, J., Tan, W., Liu, C., Zheng L., and Dang, Z., 2019, Cd^{2+} adsorption performance of tunnel-structured manganese oxides driven by electrochemically controlled redox, *Environ. Pollut*. 244:783-791. https://doi.org/10.1016/j.envpol.2018.10.062.

Liu, T., Lawluvy, Y., and Shi, Y., 2022, Adsorption of cadmium and lead from aqueous solution using modified BC: a review, *J. Environ. Chem. Eng*. 10:106502. http://dx.doi.org/10.1016/j.jece.2021.106502.

Ragadhita R., and Nandiyanto A., 2021, How to Calculate Adsorption Isotherms of Particles Using Two-Parameter Monolayer Adsorption Models and Equations, Indones. J. Sci. Technol. 6:205-234. http://dx.doi.org/10.17509/ijost.v6i1.32354.

Redlich, O.J., and Peterson, D.L., 1959, Useful adsorption isotherm, *J. Phy. Chem*. 63:1024. http://dx.doi.org/10.1021/j150576a611.

Sabando-Fraile, C., Corral-Bobadilla, M., Lostado-Lorza, R., and Cabredo-Pinillos, S., 2024, A synergistic integration of life cycle assessment and response surface methodology to optimize grape stalk waste-based biosorption for effective Cd(II) removal, *J. Clean. Prod*. 450:141938. https://doi.org/10.1016/j.jclepro.2024.141938.

Sahoo, U.K., Lalremruata, J., and Lalramnghinglova, H., 2014, Assessment of fuelwood based on community preference and wood constituent properties of tree species in Mizoram, north-east India, *For. Trees Livelihood*. 23:280-288. http://dx.doi.org/10.1080/14728028.2014.943684.

Suya, M., Shuaixian, M., Jinshuai, S., Jiacheng, Z., Jiale, Z., Yingchao, L., Xinrong, W., Zizhen, M., and Caihong, Y., 2024, Exploring the synergistic interplay of sulfur metabolism and electron transfer in Cr(VI) and Cd(II) removal by *Clostridium thiosulfatireducens*: Genomic and mechanistic insights, *Chemosphere*. 352:141289. https://doi.org/10.1016/j.chemosphere.2024.141289.

Temkin, M.I., and Pyzhev, V., 1940, Kinetics of ammonia synthesis on promoted iron catalyst, *Acta USSR*. 12:327–356.

Zamri, M.F.M.A., Kamaruddin, M.A., Yusof Sf, M.S, Aziz, H.A., and Foo, K.Y., 2017, Semi-aerobic stabilized landfill leachate treatment by ion exchange resin: isotherm and kinetic study, *Appl. Water Sci*. 7:581-590. http://dx.doi.org/10.1007/s13201-015-0266-2.

Table 1. Different adsorption isotherm models with their Parameters for the adsorption of Cd(II) onto biochar

Isotherm	Parameter	Value
Freundlich	K_f	9.204 mg/g
	n	2.98
	R^2	0.907
Langmuir	q_{max}	28.57 mg/g
	B	0.34
	R^2	0.993
Temkin	A_T	4.69 L/g
	b_T	461.8 J/mol
	b_T	≈0.11 kcal/mol
	R^2	0.958
Redlich-Peterson	K_{RP}	9.89
	a_{RP}	0.330
	β	1.01
	R^2	0.999
Sips	q_m	27.04 mg/g
	K_{LF}	0.39
	n	1.05
	R^2	0.991
Flory-Huggins	K_{FH}	0.0039 L/mol
	n_{FH}	-1.48
	R^2	0.986
	ΔG^o	-13.86 kJ/mol
Fowler-Guggenheim	K_{FG}	4.02×10^{-4} L/mg
	W	-12.04 kJ/mol
	R^2	0.99
Harkin-Jura	*A*	142.85
	B	1.57
	R^2	0.761

Table 2. Different adsorption Kinetic models with their Parameters for the adsorption of Cd(II) onto biochar

Kinetic	Parameter	Value
Pseudo-first-order	q_e	13.03 mg/g
	k_1	39.15×10^{-3}/min
	R^2	0.979
Pseudo-second-order	k_2	6.42×10^{-3} g/mg/min
	q_e	16.66 mg/g
	R^2	0.999

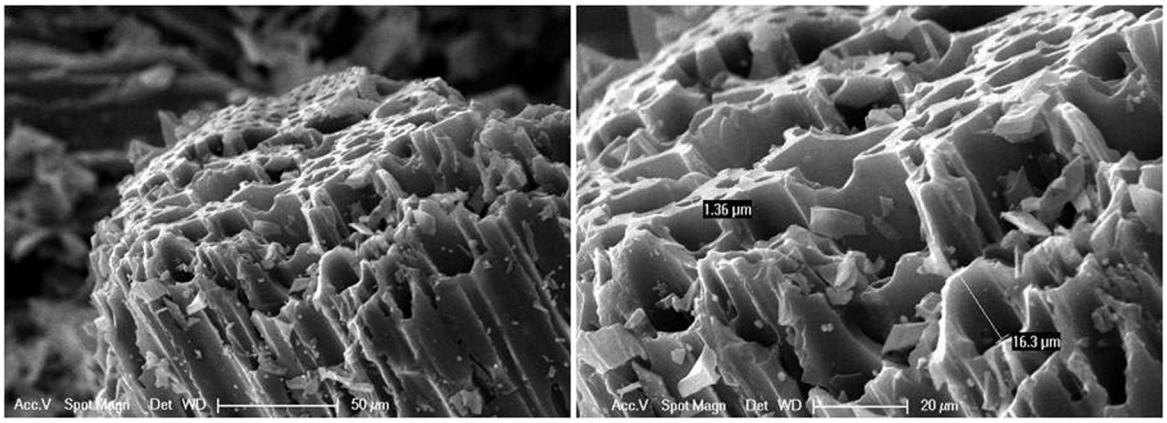

Fig. 1. SEM micrograph revealing the present of different pores on the surface of wood biochar.

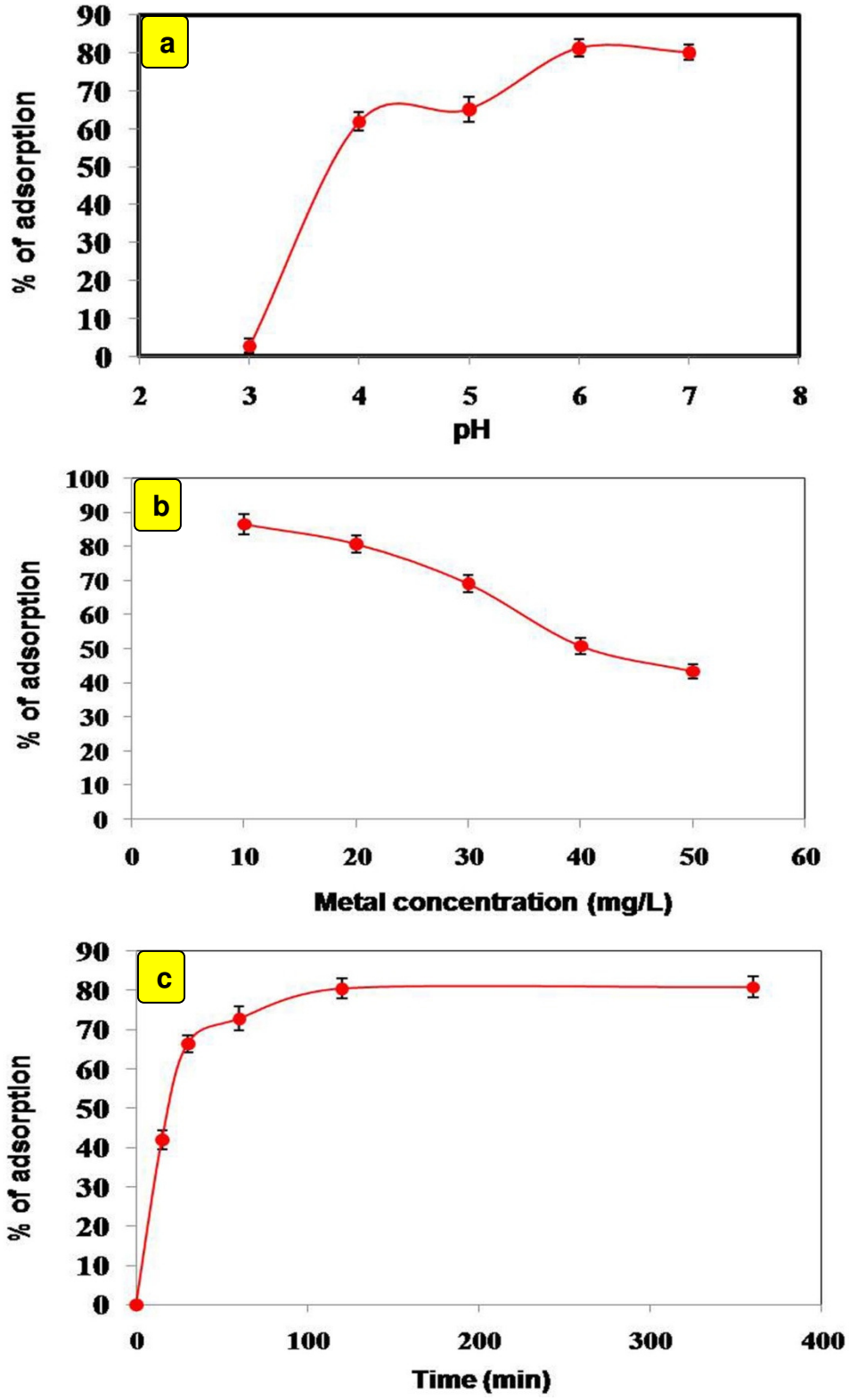

Fig. 2. Effect of (**a**) pH; (**b**) Initial metal concentration; and (**c**) time of contact on the sorption of Cd(II) onto Biochar.

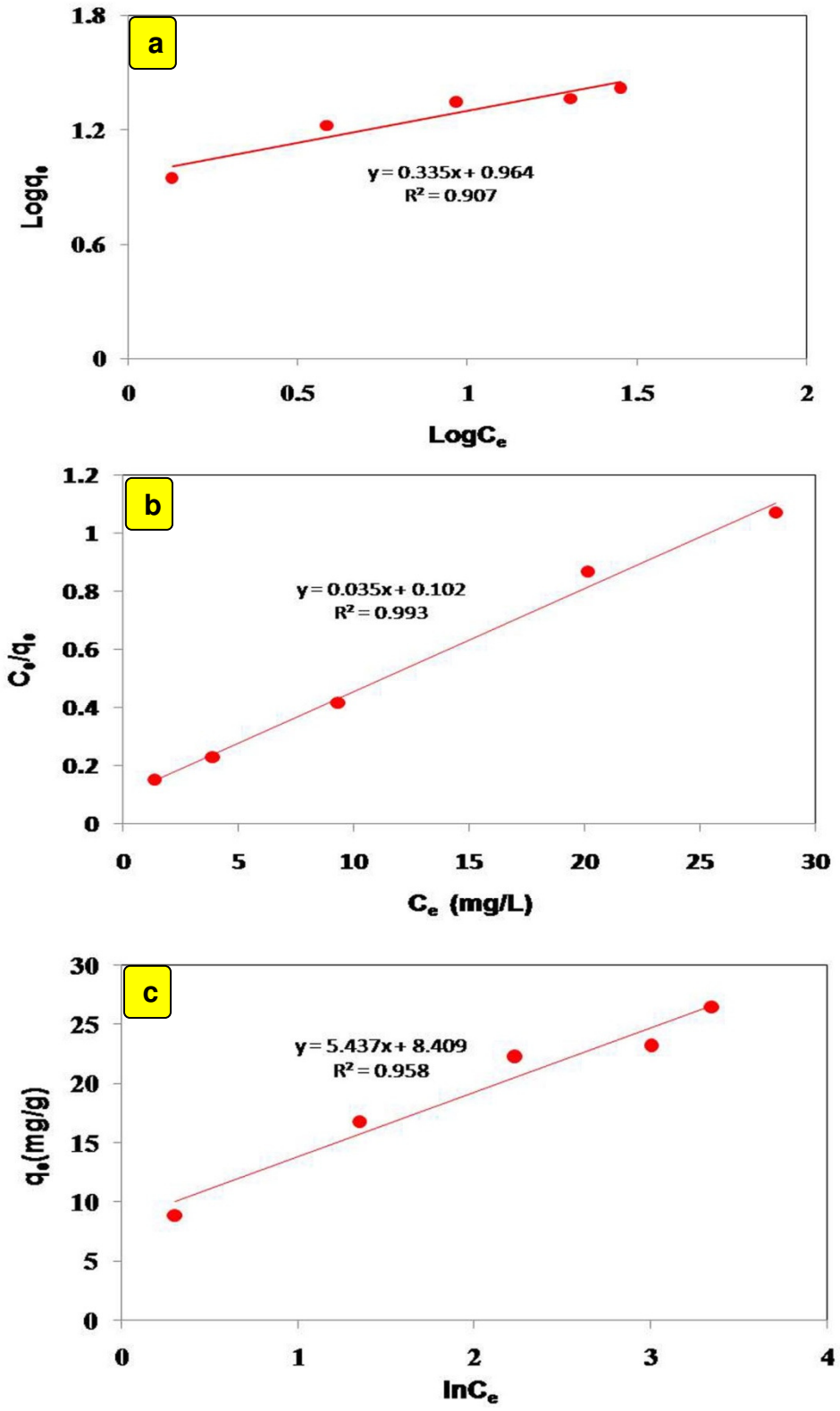

Fig. 3. Isotherms studies (**a**) Freundlich isotherm; (**b**) Langmuir; and (**c**) Temkin isotherm for Cd(II) adsorption onto wood biochar.

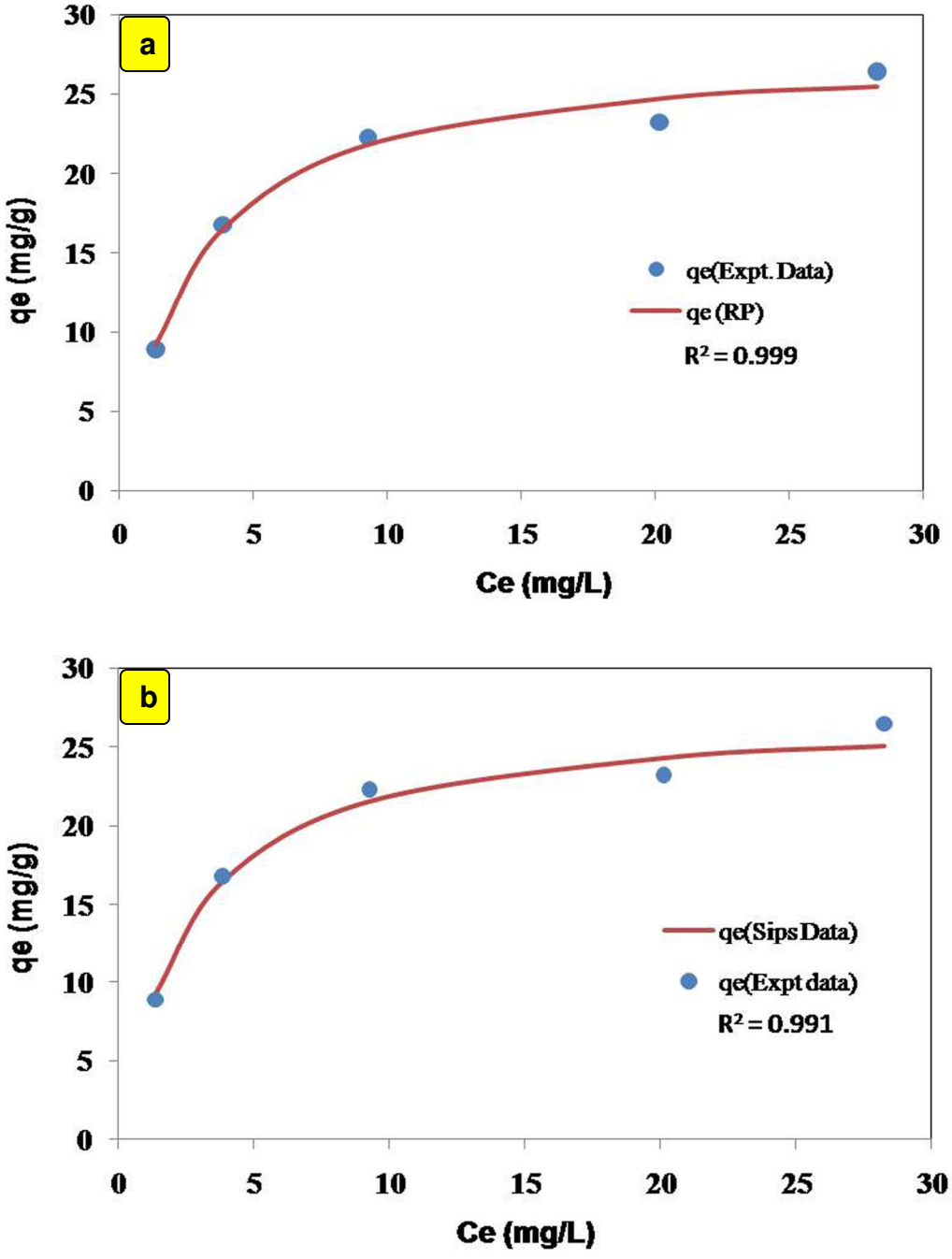

Fig. 4. Isotherms studies (**a**) Redlich - Peterson (R-P) isotherm; and (**b**) Sips isotherm model for Cd(II) adsorption onto wood biochar.

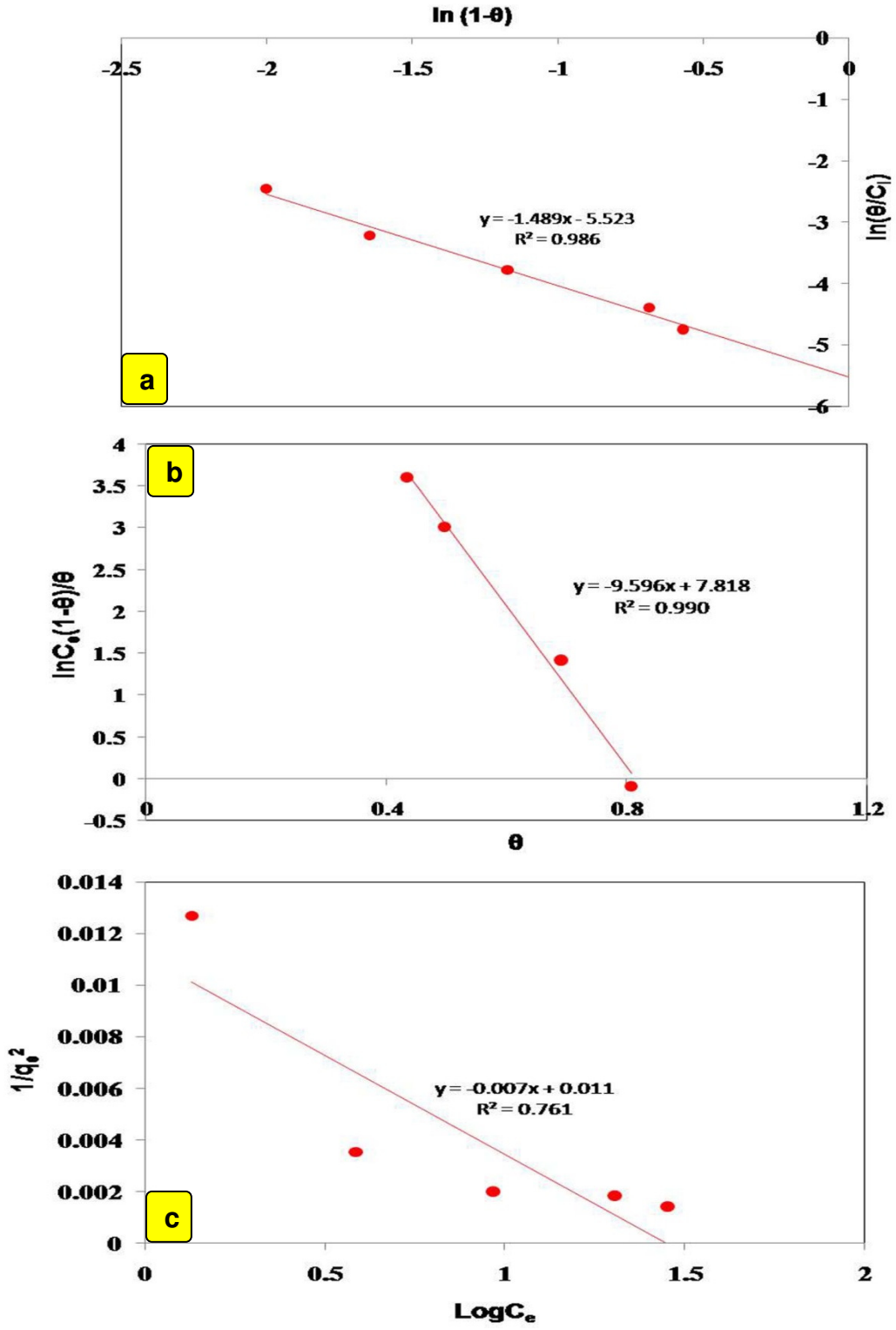

Fig. 5. Isotherms studies (**a**) Flory-Huggins isotherm; (**b**) Fowler–Guggenheim isotherm; and (**c**) Harkin-Jura isotherm model for Cd(II) adsorption onto wood biochar

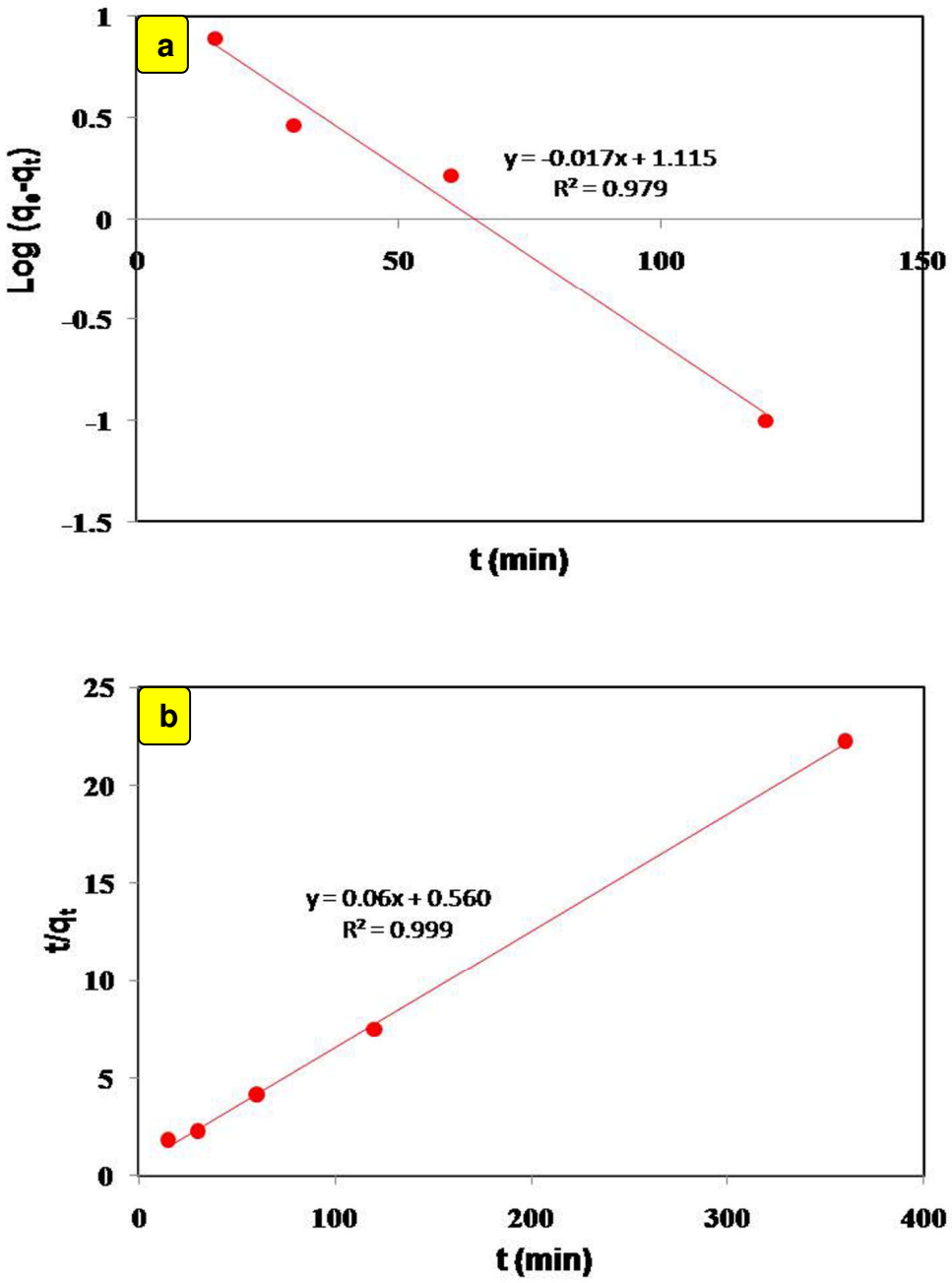

Fig. 6. (**a**) Pseudo-first–order kinetic; and (**b**) Pseudo-second–order kinetics for the adsorption of Cd(II) onto wood biochar.